

Velocity fluctuations in cooling granular gases.

Andrea Baldassarri¹, Umberto Marini Bettolo Marconi², and Andrea Puglisi³

¹ INFM Udr Roma 1, University of Rome “La Sapienza”, piazzale Aldo Moro 2, I-00185, Roma, Italy

² Dipartimento di Matematica e Fisica and INFM Udr Camerino, University of Camerino, Via Madonna delle Carceri I-62032 Camerino, Italy

³ INFM Center for Statistical Mechanics and Complexity, University “La Sapienza”, piazzale Aldo Moro 2, I-00185 Roma, Italy

Summary. We study the formation and the dynamics of correlations in the velocity field for 1D and 2D cooling granular gases with the assumption of negligible density fluctuations (“Homogeneous Velocity-correlated Cooling State”, HVCS). It is shown that the predictions of mean field models fail when velocity fluctuations become important. The study of correlations is done by means of molecular dynamics and introducing an Inelastic Lattice Maxwell Models. This lattice model is able to reproduce all the properties of the Homogeneous Cooling State and several features of the HVCS. Moreover it allows very precise measurements of structure functions and other crucial statistical indicators. The study suggests that both the 1D and the 2D dynamics of the velocity field are compatible with a diffusive dynamics at large scale with a more complex behavior at small scale. In 2D the issue of scale separation, which is of interest in the context of kinetic theories, is addressed.

1 Introduction

The inelastic hard spheres model [1] without energy input, initially prepared in a homogeneous state, exhibits, after a rapid transient, a regime characterized by homogeneous density and a probability distribution of velocities that depends on time only through the total kinetic energy (global granular temperature $T_g(t)$), i.e. a scaling velocity distribution. This is the so called *Homogeneous Cooling State* (HCS) or Haff regime [2]. It has been shown by several authors [3–6] that this state is unstable with respect to shear and clustering instabilities: structures can form that seem to minimize dissipation, mainly in the form of velocity vortices and high density clusters. These instabilities grow on different space and time scales, so that one can investigate them separately. Several theories have been proposed to take into account the emergence of structures in granular gases. Some of these are more fundamental, because derive the correlation functions directly from the kinetic equations [7]; others, that assume the validity of the hydrodynamic description, deserve the name of mesoscopic theories [8]; others are phenomenological theories that suggest analogies with Burgers equation [9,10] or spinodal decomposition models [11] or mode coupling theories [12]. Some of these theories can describe the behavior of the cooling granular gas far deeply into the

correlated regime, giving predictions for the asymptotic decay of energy. In this paper, after a brief summary of the results of these theories, we show how the departure from the HCS can be well modeled by a class of models obtained placing on a lattice the original homogeneous Inelastic Maxwell Model. These models have the disadvantages of being conceived under the assumption of negligible density fluctuations and therefore can be useful only in the description of the first instability, i.e. the growth of velocity fluctuations. In section 2 we review the HCS, its instabilities and the existing theories. In section 3 we briefly discuss the Inelastic Maxwell Model [13–15], which is a starting point for the introduction of the Inelastic Lattice Maxwell Models (ILMM). In section 4 and in section 5 the analysis and results of the ILMM in one and two dimensions are reviewed [14,16]. Finally in section 6 conclusions are drawn.

2 Instabilities of the Homogeneous Cooling State

A cooling granular gas in d dimensions is defined as an ensemble of N grains, i.e. hard objects (rods if $d = 1$, disks if $d = 2$, spheres if $d = 3$) of linear size (diameter) σ , placed in a volume V with periodic boundary conditions. The grains evolve freely and interact with each other through instantaneous binary inelastic collisions. The rule that gives the velocities after the collision as functions of the velocities before the collision is the definition of the particular granular gas model. In this case we use the model with constant restitution coefficient without rotational degrees of freedom and set the mass of the grains $m = 1$. Other models have been considered in the literature [1]. The collision rule between a particle with velocity \mathbf{v} and one with velocity \mathbf{v}^* for this model is:

$$\mathbf{v}' = \mathbf{v} - \frac{1+r}{2} [(\mathbf{v} - \mathbf{v}^*) \cdot \hat{\mathbf{n}}] \hat{\mathbf{n}} \quad (1)$$

where the primed velocity is the post-collisional one, $\hat{\mathbf{n}} = (\mathbf{r} - \mathbf{r}^*)/|\mathbf{r} - \mathbf{r}^*|$ is the unit vector in the direction joining the centers of colliding particles, and r is the restitution coefficient and takes values between 0 and 1. When $r = 1$ the collision is elastic.

Usually (in numerical or real experiments) granular gases are prepared in a homogeneous situation: uniform-random positions of grains, Gaussian or uniform-random initial velocity with no preferred direction. It happens that, if the system is large enough or the inelasticity large enough, the imposed homogeneity is broken after a certain time. The more accepted scenario is a two time homogeneity breaking: at a time t_s the velocity field becomes unstable to the formation of shear bands, then at a time $t_c > t_s$ the density field becomes unstable toward the formation of high density clusters.

2.1 The homogeneous cooling state

A granular gas evolving from a homogeneously random state loses memory of its initial condition after a time of the order of one collision per particle and rapidly enters the Homogeneous Cooling Regime. This regime is expected to be well described by the granular Boltzmann Equation (see for example [7]). This means that in this regime the total probability density function (p.d.f.) at collision is factorisable in one-particle p.d.f.'s: $p_N(\mathbf{r}_1 \dots \mathbf{r}_N, \mathbf{v}_1 \dots \mathbf{v}_N, t) = \prod_{i=1}^N p_1(\mathbf{r}_i, \mathbf{v}_i, t)$.

The kinetic definition of HCS is given by the homogeneity ansatz plus the scaling ansatz for the one particle distribution function:

$$p_1(\mathbf{r}, \mathbf{v}, t) = \frac{1}{V} P(\mathbf{v}, t) = \frac{1}{V v_0^d(t)} \tilde{P}(\mathbf{c}) \quad (2)$$

where $\mathbf{c} = \mathbf{v}/v_0(t)$ and $v_0(t)$ is the thermal velocity defined by $T(t) = v_0^2(t)/d$ with $T(t)$ the granular temperature; here we have assumed that $\int d\mathbf{v} \int d\mathbf{r} p_1 = 1$ and also that $\int d\mathbf{v} P = 1$. If the Eq. (2) is inserted in the Boltzmann Equation an equation for the temperature is obtained:

$$\frac{dT}{dt} = -2\omega\gamma T \quad (3)$$

where ω is the time dependent collision frequency, while γ is the time independent cooling rate. These two functions can be approximated, using the Maxwellian approximation $\tilde{P} \approx (\frac{2\pi}{2})^{-d/2} \exp(-\frac{d\mathbf{c}^2}{2})$, by ω_0 and γ_0 :

$$\omega_0 \propto \sqrt{T} \quad (4a)$$

$$\gamma_0 = \frac{1-r^2}{2d}. \quad (4b)$$

In this case the solution of the temperature equation (3) reads:

$$T(t) = \frac{T(0)}{(1 + \gamma_0 t/t_0)^2} = T(0) \exp(-2\gamma_0 \tau) \quad (5)$$

where $t_0 = 1/\omega(T(0))$ is the mean free time at the initial temperature $T(0)$ and

$$\tau = \frac{1}{\gamma_0} \ln(1 + \gamma_0 + t/t_0) \quad (6)$$

is the cumulated collision number obtained from the definition $d\tau = \omega(T(t))dt$. Eq. (5) is known as Haff's law [2].

Corrections to the constants appearing in eq. (5) stem from a more careful consideration of the HCS: when the volume fraction is non negligible the Enskog-Boltzmann equation should be employed instead of Boltzmann equation. This is identical to the Boltzmann equation but for a multiplicative

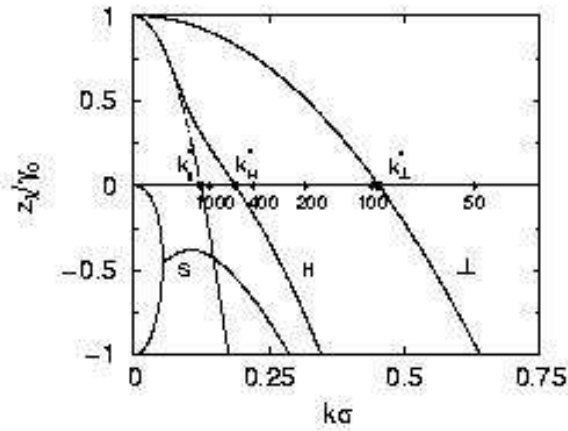


Fig. 1. Growth rates ζ_λ/γ_0 for shear ($\lambda = \perp$), heat ($\lambda = H$) and sound ($\lambda = \pm$) modes versus $k\sigma$ for inelastic hard disks with $r = 0.9$ at a packing fraction $\phi = 0.4$. The dashed line indicate the imaginary parts of the sound modes. Here σ is the diameter of a particle. (From Orza et al. [19])

constant in the collision integral that takes into account static density correlations due to the fact that the gas is not perfectly dilute. Very recently it has been shown [17] that there are also small velocity correlations which must be considered and that modify the molecular chaos hypothesis: with this correlations the law $T \sim t^{-2}$ is still valid but more precise corrections to the constant γ_0/t_0 appear.

The Haff law can be also derived in the framework of granular hydrodynamics [18,6]: in the HCS hydrodynamics can be considered valid as a consequence of homogeneity of the density and velocity field and of the slow temperature decay. The evolution of the (space uniform) temperature field is exactly the same as in eq. (5).

2.2 Instabilities of the homogeneous cooling state

Kinetic arguments, linear stability analysis of hydrodynamic equations and numerical simulations lead to the evidence that the HCS is unstable. In particular, it has been shown that large scale fluctuations of velocity and density can grow exponentially breaking the homogeneity of the system. The fact that the fluctuations arise at large scale means that, if the system is small enough, the HCS lasts forever. Moreover the minimum scale of formation of fluctuations depends upon inelasticities and is smaller at larger inelasticities: this means that for a quasi-elastic gas it is necessary to take a very large volume to observe the breaking of homogeneity.

The linear stability analysis of hydrodynamics gives a good description of the instability of fluctuations. The procedure is applied to the fields rescaled with respect to the Homogeneous Cooling State, i.e. $\tilde{n} = n(\mathbf{r}, t)/n$ (being n the average density), $\tilde{\mathbf{u}}(\mathbf{r}, t) = \mathbf{u}(\mathbf{r}, t)/\sqrt{T(t)}$ and $\tilde{T}(\mathbf{r}, t) = T(\mathbf{r}, t)/T(t)$, and therefore any instability or emerging structure is not absolute but relative to this decaying reference state. Moreover the instabilities are studied in \mathbf{k} space (the space of Fourier modes) and, when $d > 1$, the velocity field is decomposed in a parallel component $\tilde{\mathbf{u}}_{\parallel}(\mathbf{k}, t)$ and in $d - 1$ orthogonal components $\tilde{\mathbf{u}}_{\perp}(\mathbf{k}, t)$ with respect to the vector \mathbf{k} . In figure 1 we report the results of such an analysis, taken from the literature [19]. This analysis shows that the evolution of fluctuations of normal velocity components (shear modes, $\tilde{\mathbf{u}}_{\perp}$) are not coupled with any other fluctuating component. At the same time, the remaining components are coupled together. The rate of decay/growth for the shear mode reads $\zeta_{\perp}(k) = \gamma_0(1 - k^2\xi_{\perp}^2)$ where ξ_{\perp} depends on the transport coefficients appearing in the hydrodynamics. We refer to [8] for detailed calculations of this correlation length. At low values of k (in the so-called “dissipative range”) also the heat mode is “pure”, as it is given by the longitudinal velocity mode $\tilde{\mathbf{u}}_{\parallel}$ only, with eigenvalue $\zeta_H(k) \simeq \gamma_0(1 - \xi_{\parallel}^2 k^2)$; in this range the sound modes are combination of density and temperature fluctuations. The most important result of this analysis is that $\zeta_{\perp}(k)$ and $\zeta_H(k)$ are *positive* below the threshold values $k_{\perp}^* = 1/\xi_{\perp} \sim \sqrt{\epsilon}$ and $k_H^* \simeq 1/\xi_{\parallel} \sim \epsilon$ respectively, indicating two linearly unstable modes with exponential (in τ , i.e. the time measured by the cumulated number of collisions per particle) growth rates. Here we have used the notation $\epsilon = 1 - r^2 \equiv 2d\gamma_0$.

The shear and heat instabilities are well separated at low inelasticity (i.e. low ϵ), as $k_{\perp}^* \sim \sqrt{\epsilon}$ while $k_H^* \sim \epsilon$, so that $k_{\perp}^* \gg k_H^*$. It is also important to note that the linear total size L of the system can suppress the various instability, because the minimum wave number $k_{min} = 2\pi/L$ can be larger than k_H^* or even than k_{\perp}^* .

When fluctuations grow, structures emerge. In molecular dynamics simulations these structure appear as shocks in $d = 1$, or vortices and clusters in $d = 2$. In $d > 2$, a detailed analysis of structure factors (from fluctuating hydrodynamics [8] or ring kinetic theory [7]) has established that all the main correlation lengths (which indicate the typical size of structures *in the rescaled fields*) should grow as $\sim \tau^{1/2}$. In particular this is expected for the size of vortices $L_v \sim \tau^{1/2}$ and the size of clusters $L_{cl} \sim (\tau/\epsilon)^{1/2}$: this again shows that, at small inelasticities ϵ , the size of clusters grows more slowly than that of vortices.

2.3 Conjectures

After a brief transient during which the instabilities grow exponentially in τ with the rates given above, the description suggested by linear stability analysis ceases to be meaningful. Molecular dynamics (MD), in the absence of experiments (the cooling granular gas being a reference model and not a real

system), are the more reliable tools, but they are very cpu-time consuming: to obtain a decent statistics of the asymptotic dynamics of a granular gas, large enough to observe instabilities, MD simulations must be carried on for days. To our knowledge a definitive clear picture of the asymptotics of this model is still lacking (with month-lasting simulations Isobe [20] has obtained what he called the “final state”, which resembles 2D turbulence, but this was done in a quasi-elastic limit).

On the other side there are effective models that can grasp the essence of the phenomena with particular assumptions. Here we rapidly review some of these:

- Brito and Ernst have shown by means of a mode-coupling [12] theory that the asymptotic energy decay should follow a diffusive form $\sim \tau^{-d/2}$.
- Wakou et al. [11] have demonstrated that the evolution of the flow field of a granular fluid, neglecting the convective term $\mathbf{u} \cdot \nabla \mathbf{u}$, can be cast in the form of a Time Dependent Ginzburg-Landau equation for a non-conserved order parameter. The energy functional has a *continuous* set of degenerate minima, having the shape of a Mexican hat. When the convective term is added, only subsets of admissible solutions are selected out of this infinite set of minima. In two dimensions only *two* distinct minima survive: therefore the $d = 2$ cooling granular gas, during the formation of instabilities, greatly resembles the spinodal decomposition for a non-conserved order parameter (Model A universality class, in the Hohenberg-Halperin classification [21]).
- Ben-Naim et al. [9] have studied the cooling granular gas in $d = 1$, discovering that, after the homogeneous (Haff) phase, it asymptotically becomes independent of the value of inelasticity ϵ and maps onto the sticky gas model. For such a sticky gas the asymptotic temperature decay is proportional to $t^{-2/3}$, when density clusters and velocity shocks form. The velocity field of the sticky gas [22] is described by the inviscid limit of the Burgers equation [23]. The relation to the Burgers equation is useful to establish an estimate of the tails of the asymptotic velocity distribution $P(v, t) \sim t^{1/3} \Phi(vt^{1/3})$ (independent of r), which reads $\Phi(z) \sim \exp(-|z|^3)$. The MD simulations have revealed only slight deviations from the Gaussian, and the authors have imputed the discrepancy from the expected behavior to the smallness of the constant in front of $|z|^3$. More recently it has been conjectured [10] that the Burgers equation describes the flow velocity $\mathbf{u}(\mathbf{r}, t)$ of a cooling granular gas for arbitrary values of the inelasticity ϵ in generic d dimensions. This conjecture implies that the asymptotic behavior of the cooling inelastic gas is independent of ϵ (as it always falls in the universality class of the sticky gas) and that the upper critical dimension for the disappearance of the inelastic collapse is $d_c = 4$. However MD simulations in $d > 4$ seem to show that the shear instability and the inelastic collapse do not disappear [24].

3 A starting point: the homogeneous Inelastic Maxwell Model

To better illustrate the analysis of the Inelastic Lattice Maxwell Models (ILMM) we start with a brief description of the homogeneous Inelastic Maxwell Model (IMM). The definition of the model is given in terms of its Boltzmann Equation, which, for scalar velocities ($d = 1$), reads:

$$\frac{\partial P(v, \tau)}{\partial \tau} + P(v, \tau) = \frac{1}{1 - \gamma^*} \int du P(u, \tau) P\left(\frac{v - \gamma^* u}{1 - \gamma^*}, \tau\right) \quad (7)$$

with $\gamma^* = (1 - r)/2$. The IMM can be introduced in different ways: (a) its Boltzmann equation can be regarded as the master equation of a simple stochastic process inspired to a model put forward by S.Ulam [25]: the process consists in the evolution of an ensemble of N velocities, at each time step (corresponding to $\Delta\tau = 2/N$, so that τ increases of 1 after averagely one collision per particle) two velocities are chosen at random with uniform distribution and are changed according to the inelastic collision rule; (b) the associated Boltzmann equation can be considered the inelastic generalization of the equation for elastic Maxwell Molecules [26,27]; (c) its Boltzmann equation can be derived from the ordinary Boltzmann equation for inelastic hard spheres assuming that the term $|v - v'|$ in the collision integral can be approximated by \sqrt{T} , as suggested by Bobylev et al. [28].

The recent surge of interest for this model has been triggered by the discovery of an exact solution [13–15] for the $d = 1$ case (eq. (7)) and the appearance of computable power law tails in the solutions of $d > 1$ cases. [29,30]. In a previous paper Ben-Naim and Krapivsky [31] showed that eq. (7) could not have a scaling solution with finite moments: in fact, a scaling form

$$P(v, \tau) \rightarrow \frac{1}{v_0(\tau)} f\left(\frac{v}{v_0(\tau)}\right) \quad (8)$$

with $v_0^2(\tau) = \int v^2 P(v, \tau) dv = E(\tau) \sim \exp(-\tau a_2)$, imposes a temporal dependence of the higher moments (if finite):

$$\langle v^{2m} \rangle = v_0(\tau)^{2m} \mu_{2m} \quad (9a)$$

$$\text{where } \mu_{2m} = \int dy f(y) y^{2m} \quad (9b)$$

does not depend on time. But they found that

$$\lim_{\tau \rightarrow \infty} \frac{\langle v^{2m}(\tau) \rangle}{(\langle v^2(\tau) \rangle)^m} = \infty. \quad (10)$$

This result does not exclude the existence of a scaling solution (8) but requires a solution with diverging moments of order $2m \geq 4$, i.e. very large

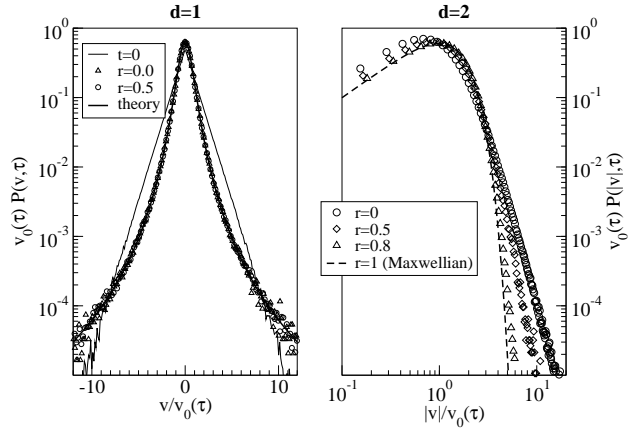


Fig. 2. Asymptotic velocity distributions $P(v, \tau)$ versus $v/v_0(\tau)$ for different values of r from the simulation of the Inelastic Maxwell Model in 1D (left) and 2D (right). In 1D the asymptotic distribution is independent of r and collapse to the Eq. (11). In 1D, the chosen initial distribution (exponential) is drawn (same result with uniform and Gaussian initial distribution). In 2D the distributions still present power-law tails, but the power depends upon r : for $r \rightarrow 1$ the pdf tends to a Maxwell distribution. Data refers to more than $N = 10^6$ particles.

algebraic tails. In this case standard methods [27] based on Fourier transform fails due to the singularity in $k = 0$ corresponding to such algebraic tails.

Remarkably, a direct inspection shows that the following velocity distribution

$$P(v, \tau) = \frac{2}{\pi v_0(\tau) \left[1 + \left(\frac{v}{v_0(\tau)} \right)^2 \right]^2} \quad (11)$$

is indeed a solution of the non-linear Boltzmann equation (7), for every value of r [13–15]. The solution (11) has the property that the moments of order $2m \geq 4$ diverge, and its Fourier transform has a singularity of the type $|k|k^2$ in $k = 0$.

We believe that eq. (11) represents the asymptotic solution for a large class of initial distributions, for the following arguments:

- as shown by Ben Naim and Krapivsky [31], the dynamics of the moments for a generic starting distribution can be computed, giving the following limit $\lim_{t \rightarrow \infty} \langle v^{2m}(t) \rangle / \langle v^2(t) \rangle^m = \infty$ for $m > 1$;
- secondly we performed numerical simulations of the BK model, collecting evidence of the convergence to the solution (11) for several starting velocity distributions, namely uniform, exponential (see figure 2, left frame) or Gaussian.

For higher dimensions, the problem of a scaling solution has been recently addressed in [10,29]. Assuming a solution with large algebraic tails, it is possible to compute the asymptotic exponent as a solution of a transcendental equation. Such equation depends explicitly on the restitution coefficient, indicating that the tail exponent varies with r (and correctly diverges for $r \rightarrow 1$, corresponding to the recovering of the Maxwell distribution for the elastic case).

A numerical observation of such algebraic tails in 2 dimensions are shown in right frame of figure 2, where a dependence on r is put in evidence. A more precise comparison of the measured exponent and the theoretical predictions are shown in figure 3. In this figure we show the results of extensive numerical simulations for the completely inelastic case ($r = 0$) of several models, in two and three dimensions.

In fact, as noted in [29], the tail exponent is in general dependent on the details of the collisions, as for instance on the distribution of the impact parameter. Two different choices have been studied in 3 dimensions, corresponding to the models denoted IMM-A and IMM-B in reference [29]: in the first model grazing collisions are favored with respect to the second one. It is interesting to notice that the analytical and numerical study confirm the existence of a scaling solution with algebraic tails, irrespectively of the collision details, but that the precise value of the exponent is not universal.

The relevance of such a scaling solution for $d > 1$ has been addressed by Bobylev *et al.* [32], who have proved the existence and the uniqueness of such an asymptotic solution (giving details on the basin of attraction).

Interesting features emerge when the inelastic Maxwell model is extended to treat grains having different physical properties, such as unequal masses, different restitution coefficients, radii, etc. The study of a binary Maxwell mixture with scalar velocities showed few unexpected properties [33,34]:

1. the kinetic temperatures of the two species are different, i.e. there is no energy equipartition, but the the ratio T_1/T_2 reaches asymptotically a constant value. Such a feature agrees with the results obtained in the framework of the Boltzmann-Enskog transport equation by Garzò and Dufty [35].
2. The velocity distributions in general differ in shape.
3. The velocity distributions have power law tails. These exponents can be calculated analytically, by a suitable generalization of a technique devised by Ernst and Brito [29]. The power law decay of cooling mixtures has been shown to vary between 2 and ∞ .

4 The one-dimensional gas

The solution of the IMM given in (11) has nothing to do with the real dynamics of a cooling granular gas in the homogeneous regime, where no algebraic

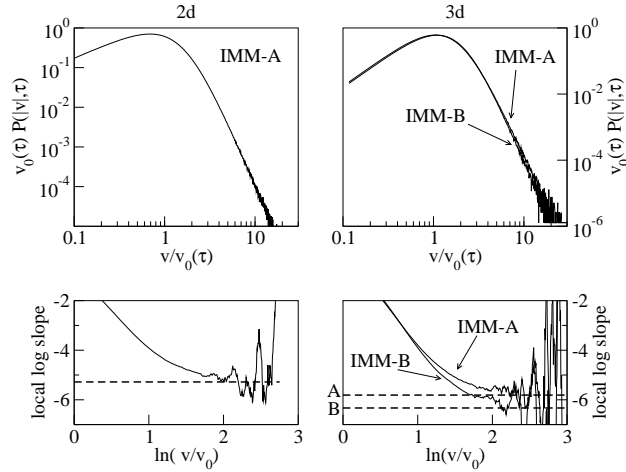


Fig. 3. Asymptotic velocity distributions $P(|v|, \tau)$ versus $|v|/v_0(\tau)$ for $r = 0$ from the simulation of the Inelastic Maxwell Model in 2D (left) and 3D (right). In 2D the asymptotic distribution tail converges to the exactly computed exponent (model IMM-A). In 3D the convergence is slower, but the difference of the predicted exponent for model IMM-A and IMM-B can be appreciated. In the bottom panels the convergences of the local logarithmic slope is put in evidence. (For the precise definition of the two models see [29].) Data refers to more than $N = 10^6$ particles.

tails appear. Instead, a good agreement (in the HCS) is found between the solution of Boltzmann equation [36] and Molecular Dynamics [37]. However we will show in the following that the Inelastic Maxwell Model with the addition of a special topology (the 1d lattice) is able to reproduce the homogeneous regime and some essential features of the first instability (enhancement of velocity fluctuations).

4.1 Molecular Dynamics

An MD simulation of N hard rods on a ring of length L shows that, besides hydrodynamic instabilities discussed above, also a kinetic singularity appears that prevents long simulation runs, the so-called “inelastic collapse” [4,38]. The inelastic collapse is the divergence of the collision rate of a small set of grains, analogous to the divergence of the collision rate of a ball left bouncing on the floor. This means that a group of particles will experience an infinite number of collisions in a finite time. To avoid such a problem, many authors [9,39] have proposed the introduction of a velocity cut-off δ such that, whenever two particles collide with a relative velocity smaller, in absolute value, than δ , the collision is elastic. Taking $\delta^2 \ll T_{min}$, being T_{min} the minimum granular temperature that one expects to observe, one can be sure that the choice of δ will not influence the main results of the simulation.

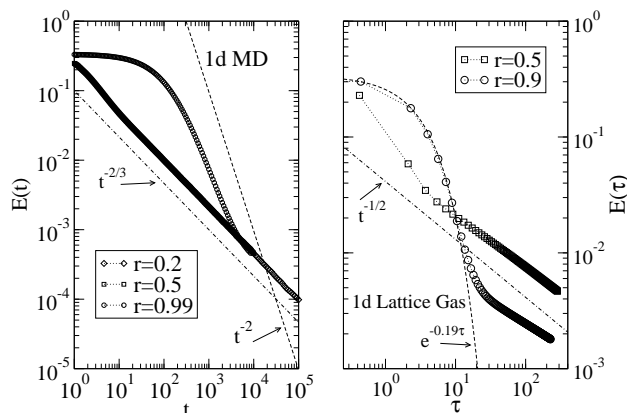


Fig. 4. Time behavior of kinetic energy for the Inelastic Hard Rods (left) and for the Inelastic Lattice Maxwell Model (right). The homogeneous Haff stage is evident only for quasi-elastic system, whereas the more inelastic ones enter almost immediately in the correlated regime. Note the different time units used (t is the physical time, defined only in MD simulations, while τ is the cumulated number of collisions per particle). The Haff law $E \sim t^{-2} \sim \exp(-\gamma_0\tau)$ is verified for both systems. The correlated regime presents a behavior $t^{-2/3}$ independent of r for the Hard Rods, while appears diffusive (in collision units) $\tau^{-1/2}$ and r -dependent for the Lattice Model. Data refer to $N = 10^6$ particles (both models).

Performing an efficient Event Driven simulation scheme (based on a tree ordering of the event times) it is possible to study easily very large systems, with $N \sim 10^6$ for thousands of collisions per particle.

In the left panel of figure 4 the decay of kinetic energy $E(t) \equiv T(t) = \langle v^2 \rangle$ is shown. It displays, for different values of r , the same behavior with two regimes: in the HCS $E(t) \sim t^{-2}$ (Haff's law), then it decays differently, i.e. $E(t) \sim t^{-3/2}$. Noticeably all the curves seem to collapse in the second regime, i.e. the asymptotic regime is equivalent (not only in the exponent, but also in the coefficients) for every value of r .

The velocity pdf's are shown in figure 5: in the HCS it appears the peculiar “two-peaks” form, which is also predicted by the study of the Boltzmann equation in the quasi-elastic limit [36]. In the second regime (which cannot be described by the Boltzmann equation, because of the presence of correlations) the pdf becomes a Gaussian.

What can be said about correlations in the second regime? An inspection of the velocity profile v_i vs. x_i (see top panel of figure 6) suggests the presence of shocks, i.e. asymmetric “discontinuities” of the velocity profile in correspondence with peaks of density (clusters). A more quantitative information about the velocity field is given by the study of the structure function $S(k, t) = \hat{v}(k, t)\hat{v}(-k, t)$ where $\hat{v}(k, t)$ is the Fourier transform of the field $v(i, t)$, presented in the left frame of figure 7. A good collapse is obtained if

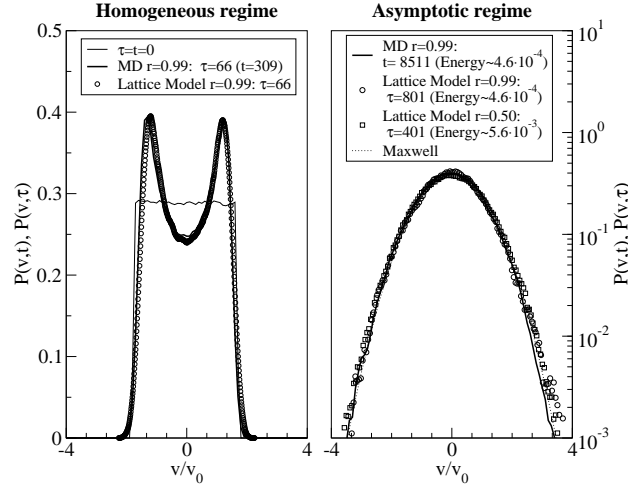


Fig. 5. Rescaled velocity distributions for the 1D MD and in the 1D ILMM, during the homogeneous (left) and the inhomogeneous phase (right). In the left frame is also shown the initial distribution (both models). The distributions refer to systems having the same energy. Data refer to $N = 10^6$ particles (both models) with $r = 0.99$ and $r = 0.5$ (for the lattice model in the inhomogeneous regime).

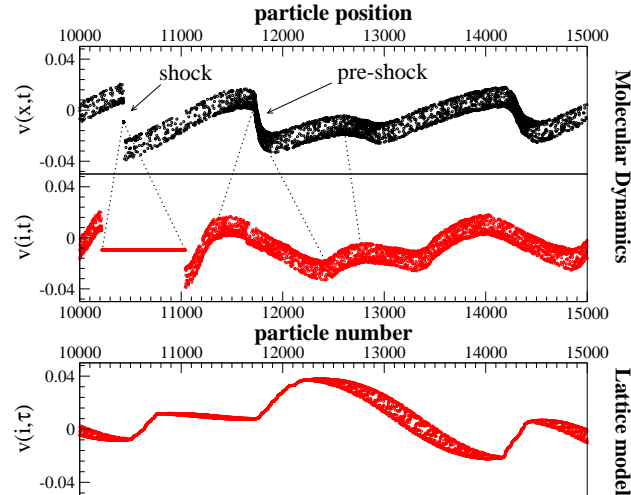


Fig. 6. Portions of the instantaneous velocity profiles for the 1D MD (top $v(x,t)$, middle $v(i,t)$) and for the 1D lattice gas model (bottom, $v(i,\tau)$). In the middle frame we display the MD profile against the particle label in order to compare the shocks and preshocks structures with the lattice gas model (the dotted lines show how shocks and preshocks transform in the two representations for the MD). Data refers to $N = 2 \cdot 10^4$ particles, $r = 0.99$ (both models).

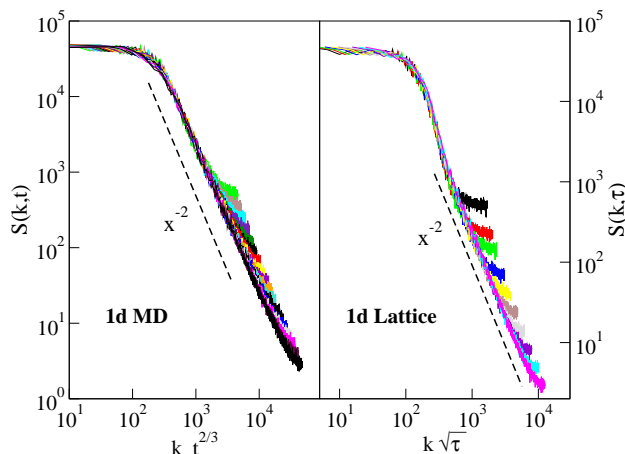


Fig. 7. Structure factors $S(k, t)$ against $kt^{2/3}$ for the 1D MD and against $k\tau^{1/2}$ for the 1D lattice gas model, in the inhomogeneous phase. Times are chosen so that the two systems have the same energies. Data refers to system with more than $N = 10^5$ particles, $r = 0.5$ (both models)

$S(k, t)$ is plotted at different times t versus $kt^{2/3} \sim k/E(t)$. The presence of short scale defects (shocks) is put in evidence by the form of structure factor at high values of k , where $S(k, t) \sim k^{-2}$: this tail of the structure function is expected, in $d = 1$, in the coarsening of a two-phases system, due to the non-analyticity (at short distances) of the spatial correlation function. This is also known as Porod law in the theory of phase ordering kinetics [40–42].

4.2 The Inelastic Lattice Maxwell Model

The Inelastic Lattice Maxwell Model in $d = 1$ is defined as follows. A set of N scalar velocities are placed on N sites on a ring. After a time $\Delta\tau = 2/N$ a couple of *neighbors* is chosen and is updated with the usual inelastic collision rule. The only constraint in the choice of the couple is that $v_i > v_{i+1}$: this is called the *kinematic constraint* and represents the physical condition necessary for a collision. It must be noted that the choice of colliding particles does not depend on the modulus of the relative velocity: this is why we consider this a “Inelastic Maxwell Model” embedded in a $1d$ lattice. In this model the only measure of time is τ , i.e. the cumulated number of collisions per particle. This makes many measures difficult to be compared with analogous MD measurements: in fact in MD simulations $\tau(t)$ depends upon the choice of δ (the elastic cut-off), while all observables depend on t independently of δ .

The analysis of the ILMM follows closely that of MD simulations and the results [13,14] are presented, in parallel, in the same figures 4, 5, 6, 7.

The study of the decay of energy (figure 4) indicates that the model well reproduces the Haff regime ($E(\tau) \sim \exp(-\gamma_0\tau)$) and displays a decay in the second regime of the form $\sim \tau^{-1/2}$.

The velocity pdf's reproduce exactly the ones measured in MD simulations (see fig. 5), showing the “two-peaks” form in the Haff stage and the Gaussian in the late stage. It must be stressed again that these features are obtained simply applying to the Inelastic Maxwell Model (which displays tails $P(v) \sim v^{-4}$) a two-neighbors (instead of N -neighbors) topology.

The inspection of velocity profiles must be carefully carried: in this model the particles cannot move and therefore a comparison with MD should be made considering v_i vs. i instead of x_i . The good agreement between MD and ILMM can be appreciated in the two bottom panels of figure 6: with this choice of abscissa, the shocks observed in MD simulations appear reversed and smoothed, very similar to the ones observed in the ILMM. Analogously the structure factor presents similar features with MD, mainly a k^{-2} behavior at high values of k (short scales) which is a signature of topological defects. In the lattice case the collapse can be obtained plotting $S(k, \tau)$ against $k\tau^{1/2}$, i.e. $\sim k/E(\tau)$ as in the MD case. We have also verified that, removing the kinematic constraint, this structure disappears and the model behaves as governed by a simple diffusion equation.

5 The two-dimensional gas

The number of interesting and realistic results obtained with the one dimensional Inelastic Lattice Maxwell Model, in spite of its extreme simplicity, convinced us to extend our study to two dimensions.

However, a smaller number of results is known from Molecular Dynamics in $d = 2$, especially in the correlated regime, which requires very long simulations. Therefore the comparison between MD and the ILMM to the case $d = 2$ is more difficult. Only recently MD simulations start to give reliable measurements even for long times, and, where possible, the comparison with our ILMM is promising.

More speculatively, we tried a series of less standard measurements with two different aims: the first is to try to understand what kind of effective equation could describe the velocity field of the ILMM; the second is to discuss some basic hypothesis necessary to a hydrodynamic description of this granular fluid. After a brief review of the known results from MD, we present the results obtained with our 2D ILMM. First the same analysis of energy decay, velocity pdf and structure factors is carried on, as in the 1d case. Moreover, to better capture the nature of the topological defects generated by the dynamics, we consider the pdf of the velocity increments. Then we present an analysis of temporal correlations, mainly aimed to identify an effective equation for the velocity field. Finally we suggest a measurement

of a hydrodynamic temperature and we sketch a discussion about the very presence of scale separation.

5.1 Known results from Molecular Dynamics

To our knowledge few MD simulations have inspected the behavior of inelastic hard disks in the late stage, i.e. after the end of Haff regime and the growth of instabilities. The departure from the homogeneity has been studied by Ernst and co-workers [6–8] and their MD simulations have shown results compatible with their predicted $\tau^{1/2}$ scaling law for the linear size of structures (vortices and clusters). A figure in a work of Huthmann et al. [43] was the first suggestion that the global velocity pdf asymptotically returns to a Gaussian (while it has fatter tails in the HCS) and recently different works on large MD simulations have confirmed this [44,10]. Recently this “return-to-the-Gaussian” scenario was put in strict relation with the presence of a Burgers-like dynamics [10]. The debate on the asymptotic energy seems to be still open, even if there are strong indications of a universal (independent of r) decay of the form $E(t) \sim t^{-1}$ [10]. A recent work of Isobe [20] demonstrates that many features of the “last” stage resemble the dynamics of 2D turbulence.

5.2 The Inelastic Maxwell Lattice Model

The ILMM in $d = 2$ is identical to that in $d = 1$ except for the fact that the particles have a 2-components vector velocity \mathbf{v}_i and that they are placed on a triangular $2D$ lattice, i.e. every particle has 6 neighbors. The dynamics is the same as in $d = 1$; the kinematic constraint here reads $(\mathbf{v}_i - \mathbf{v}_j) \cdot (\mathbf{r}_i - \mathbf{r}_j) < 0$.

The decay of energy $E(\tau)$ is shown in figure 8 for two different values of r . The Haff regime $E(\tau) \sim \exp(-\gamma_0\tau)$ is well reproduced (when $r = 0.2$ it terminates too early to be appreciated). The asymptotic decay reads $E(\tau) \sim \tau^{-1}$. Both this measurement and the decay observed in the $d = 1$ case, are compatible with a universal law $E(\tau) \sim \tau^{-d/2}$ as for a purely diffusive field.

The rescaled velocity pdf’s (see figure 9), which are initially Gaussian, become non-Gaussian in the Haff regime, with larger tails, but return Gaussian in the late stage. The analysis that follows shows that, in the late stage, the velocity field is far from being homogeneous: the global velocity pdf is strongly influenced by this homogeneity and its Gaussian form could be simply the signature of the presence of many independent domains (i.e. it is just the distribution of the average velocities of these domains).

In the figures 10 and 11 we show the presence of vortices in the velocity fields. The second figure represents the same system at a later time, demonstrating the coarsening of vortices (their number reduces and their size increases).

In $d = 2$ the structure function is defined as

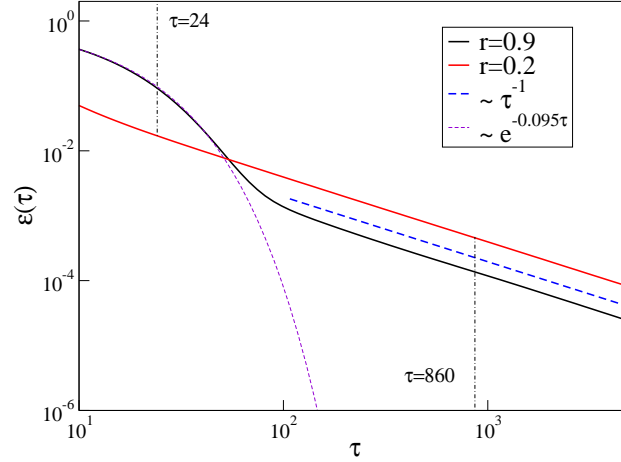


Fig. 8. Energy decay for $r = 0.9$ and $r = 0.2$ (1024^2 sites). The bold dashed line $\sim 1/\tau$ is a guide to the eye for the asymptotic energy decay, while the light dashed line is the exponential fit corresponding to the Haff law $\exp(-2\gamma_0\tau)$. The Haff regime is too short to be observed in the system with $r = 0.2$. The two indicated times $\tau = 24$ and $\tau = 860$ correspond to the plots of fig. 16.

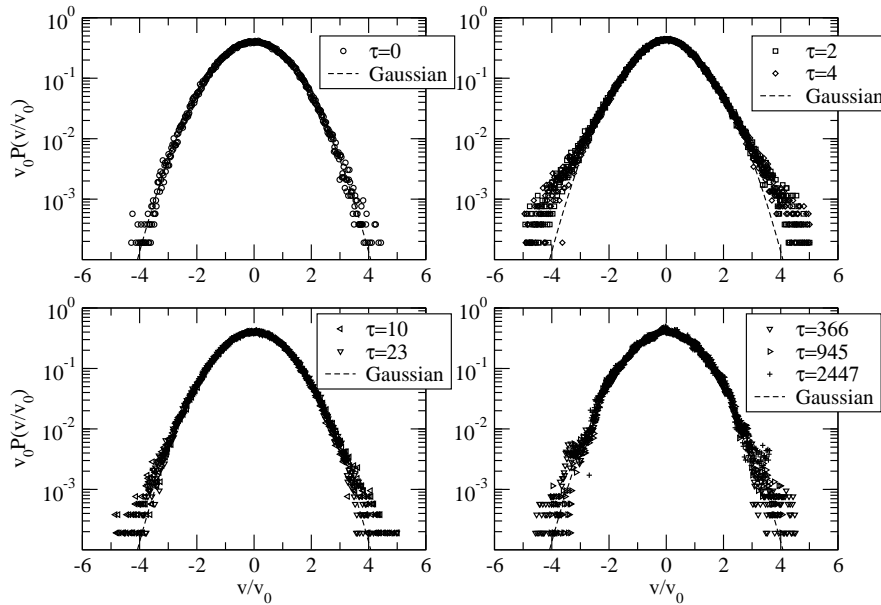


Fig. 9. Distributions of horizontal velocity at different times for the same system with $r = 0.2$ and $N = 512 \times 512$. The distributions are rescaled in order to have unit variance. The initial distribution is a Gaussian. The distribution becomes broader in the uncorrelated phase (first regime), and then turns back toward a Gaussian.

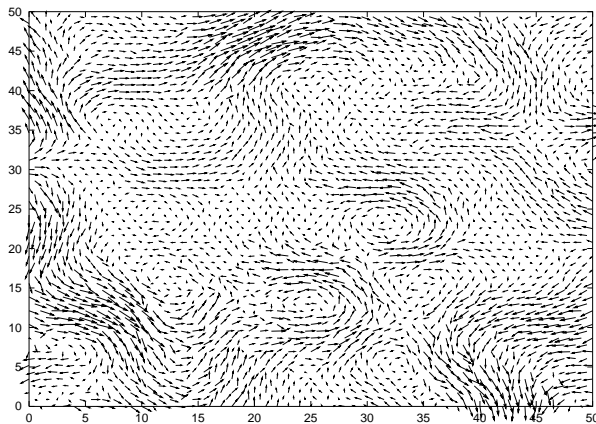


Fig. 10. A (zoomed) snapshot of the velocity field at time $\tau = 52$ for the Inelastic Lattice Gas, $d = 2$, with $r = 0.7$ and size $N = 512 \times 512$. The time has been chosen at the beginning of the correlated regime. It is evident the presence of vortices. All the velocities have been rescaled to arbitrary units, in order to be visible.

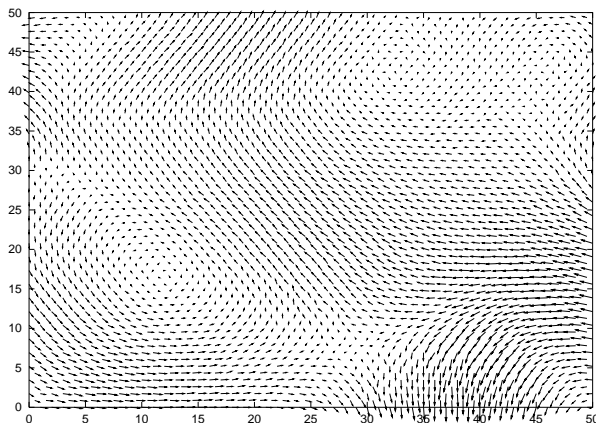


Fig. 11. Another snapshot of the same system of fig. 10 but at a later time $\tau = 535$. The diameter of the vortices has grown up. All the velocities have been rescaled to arbitrary units, in order to be visible.

$$S^{t,l}(k, t) = \sum_{\hat{k}} \mathbf{v}^{t,l}(\mathbf{k}, t) \mathbf{v}^{t,l}(-\mathbf{k}, t) \quad (12)$$

where the superscripts t, l indicate the transverse and longitudinal components of the field with respect to the wave vector \mathbf{k} and the sum $\sum_{\hat{k}}$ is over a circular shell of radius k . The analysis of the structure factor, shown in figure 12, is performed for two systems at different inelasticities. The com-

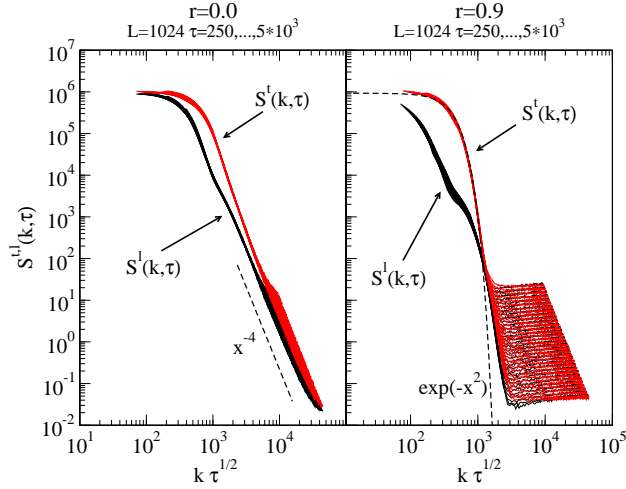


Fig. 12. Data collapse of the transverse (S^t) and longitudinal (S^l) structure functions for $r = 0$. and $r = 0.9$ (system size 1024^2 sites, times ranging from $\tau = 500$ to $\tau = 10^4$). The wave-number k has been multiplied by $\sqrt{\tau}$. Notice the presence of the plateaux for the more elastic system. For comparison we have drawn the laws x^{-4} and $\exp(-x^2)$.

mon feature is a good collapse of different time curves if plotted against $k\tau^{1/2}$ which is the signature of a domain growth (diameter of the vortices) $L(\tau) \sim \tau^{1/2}$. The elasticity however changes dramatically the other features: the more elastic system has a Gaussian structure factor at large scale (low values of k) and a plateau at small scales, i.e. quasi-elastic collisions randomize neighbour velocities while the effect of inelasticity induces a structure at large scale. The less elastic system does not present such a plateau, but a decay k^{-4} at small scales which is analogous to the Porod law [40,41] expected from the presence of defects in a phase ordering process. The difference between transversal and longitudinal component (more appreciable in the quasi-elastic system) is coherent with the theoretical analysis discussed in the introduction, which predicts an earlier and stronger correlation for the transversal component.

In the $d = 2$ ILMM we have also observed shock-like phenomena. The inspection of the distribution of longitudinal and transversal velocity differences, defined as

$$\Delta_l(\mathbf{R}, \mathbf{i}) = (\mathbf{v}_{i+R} - \mathbf{v}_i) \cdot \frac{\mathbf{R}}{R} \quad (13a)$$

$$\Delta_t(\mathbf{R}, \mathbf{i}) = (\mathbf{v}_{i+R} - \mathbf{v}_i) \times \frac{\mathbf{R}}{R} \quad (13b)$$

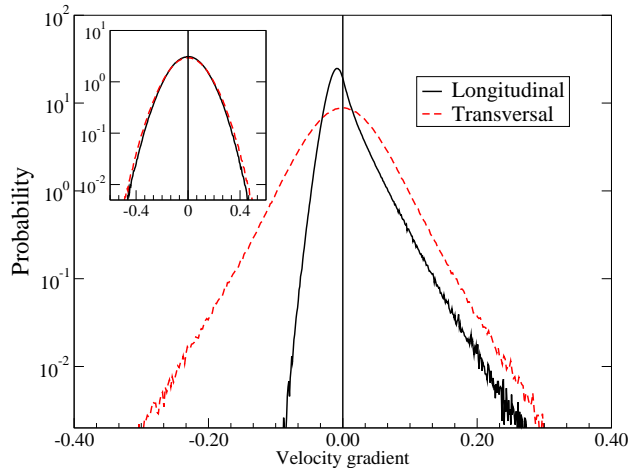


Fig. 13. Probability densities of the longitudinal and transverse velocity increments. The main figure shows the p.d.f. of the velocity differences for $R = 1$. The inset shows the Gaussian shape measured for $R = 40$ (larger than $L(t)$ for this simulation: $r = 0.2$, $t = 620$, system size 2048^2).

is contained in figure 13. The main graph shows the case $R = 1$, i.e. the distributions of gradients. Both the longitudinal and transversal components are distributed with non-Gaussian tails, but the longitudinal component presents also a strong asymmetry: this means that preferentially there are strong velocity differences in the direction of growing longitudinal velocity. This is compatible with the analysis of shocks in the bottom panels of figure 6 in the $d = 1$ case. When $R \gg 1$ the distribution of velocity differences is a Gaussian.

To better study the dynamics of the system we have calculated the two-times self-correlation of the velocity components

$$C(\tau_1, \tau_2) = \frac{\sum_i v_i(\tau_1)v_i(\tau_2)}{N} \quad (14)$$

During a short time transient, the self-correlation function of our model depends on $\tau_1 - \tau_2$, i.e. it is time translational invariant (*TTI*). Later, $C(\tau_1, \tau_2)$ reaches an “aging” regime and depends only on the ratio $x = \tau_1/\tau_2$. This *TTI* transient regime is similar to what occurs during the coarsening process of a quenched magnetic system: the self-correlation of the local magnetization $a(\tau_w, \tau_w + \tau)$ for $\tau \ll \tau_w$ shows a *TTI* decay toward a constant value $m_{eq}^2(T_{quench})$ that is the square of the equilibrium magnetization, indicating that the local magnetization is evolving in an ergodic-like fashion. Thereafter the self-correlation decays with the *aging* scaling law indicated above. Obviously, when $T_{quench} \rightarrow 0$, the *TTI* transient regime disappears. In our model the behavior of the self-correlation is even more subtle, as the cooling process imposes a (slowly) decreasing “equilibrium” temperature $T_{quench} \rightarrow 0$:

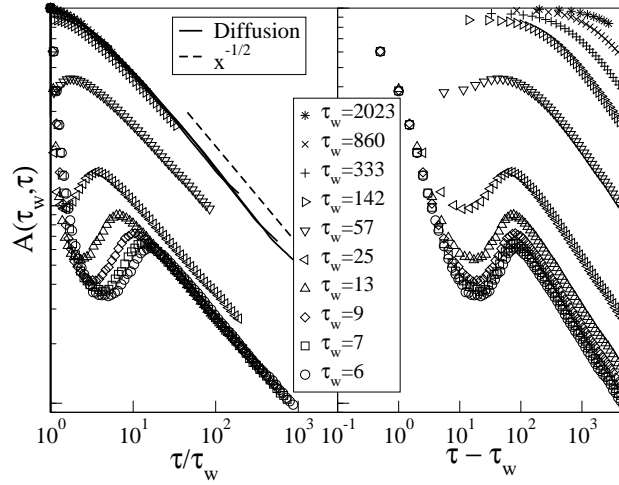


Fig. 14. Angular auto-correlation function $A(\tau, \tau_w)$ for different values of the waiting time τ_w and $r = 0.9$ (1024^2 sites). The graph on the left shows the convergence to the τ/τ_w diffusive scaling regime, for large τ_w . For small τ_w , a local minimum is visible (for such a quasi elastic dynamics). In the graph on the right the same data are plotted vs $\tau - \tau_w$: note that the small τ_w curves tend to collapse. For higher τ_w the position of the local minimum does not move sensibly, but its value grows and goes to 1 for large τ_w

this progressively erodes the *TTI* regime and better resembles a finite rate quench. The same dependence on the *TTI* manifests itself in the angular auto-correlation, shown in figure 14:

$$A(\tau, \tau_w) = \frac{1}{N} \sum_i \cos(\theta_i(\tau_w + \tau) - \theta_i(\tau_w)). \quad (15)$$

The non-monotonic behavior of $A(t, t_w)$ suggests that the initial direction of the velocity induces a change in the velocities of the surrounding particles, which in turn generates, through a sequence of correlated collisions, a kind of retarded field oriented as the initial velocity. As t_w increases the maximum is less and less pronounced.

The behavior of the energy decay ($E(\tau) \sim \tau^{-d/2}$), the law of growth of domains ($L(\tau) \sim \tau^{1/2}$) and the “aging” form of the two-times self-correlations, as well as the Gaussian velocity pdf’s and the Gaussian form at large scale in the structure factors, are strong evidence that the model behaves similarly to a system governed by the diffusion equation:

$$\frac{\partial \phi_i}{\partial \tau} = D \sum_j \frac{\partial^2 \phi}{\partial r_j^2} \quad (16)$$

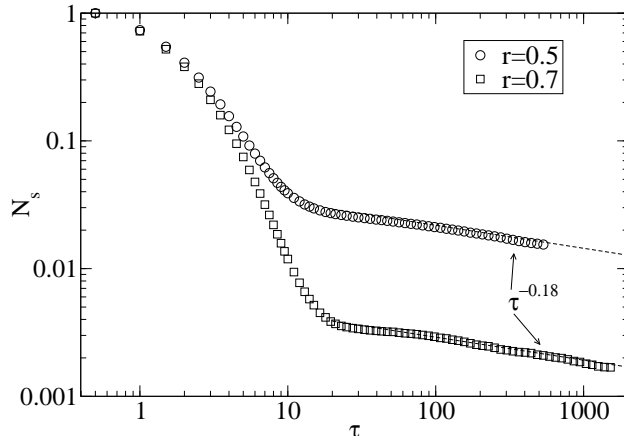


Fig. 15. Measure of the persistence of the Inelastic Lattice Gas in $d = 2$, for two different values of the restitution coefficient. The power-law regime corresponds to the correlated regime. The measured exponent $\theta = 0.18$ is, with this precision, equal to the persistence exponent numerically measured in the diffusive dynamics.

where ϕ is a suitable field depending on the velocity field (it could be a scalar, for example the z -component of the vorticity field $\nabla \times \mathbf{v}$).

To perform a further check of this conjecture, we have measured the persistence exponent [45] of the model, which is very sensitive to the class of universality. We have counted the number $N_s(\tau)$ of sites where the x velocity component never changed sign from the starting time of the dynamics up to time τ . In the correlated regime we observe $N_s(\tau) \sim \tau^{-\theta}$ with $\theta = 0.18$ which is equal, up to this precision, to the persistence exponent numerically measured for the diffusive dynamics.

In the spirit of verifying the possibility of a hydrodynamic (mesoscopic) description of this model, we have also analysed the average local granular temperature T_σ , defined as:

$$T_\sigma = \langle |\mathbf{v} - \langle \mathbf{v} \rangle_\sigma|^2 \rangle_\sigma \quad (17)$$

where $\langle \dots \rangle_\sigma$ means an average on a region of linear size σ .

If we call $L(t)$ a characteristic correlation length of the system, since when $\sigma \gg L(t)$ the local average tends to the global (zero) momentum, then $\lim_{\sigma \rightarrow \infty} T_\sigma = E$. For $\sigma < L(t)$, instead, $T_\sigma < E$. The behavior of T_σ in the uncorrelated (Haff) regime and in the correlated (asymptotic) regime for two different values of r is presented in figure 16. For quasi elastic systems T_σ exhibits a plateau for $1 \ll \sigma \ll L(t)$ that identifies the strength of the internal noise (see also the plateau in the structure factor, figure 12) and indicates the mesoscopic scale necessary for a hydrodynamics description. The local temperature ceases to be well defined for smaller r , revealing an

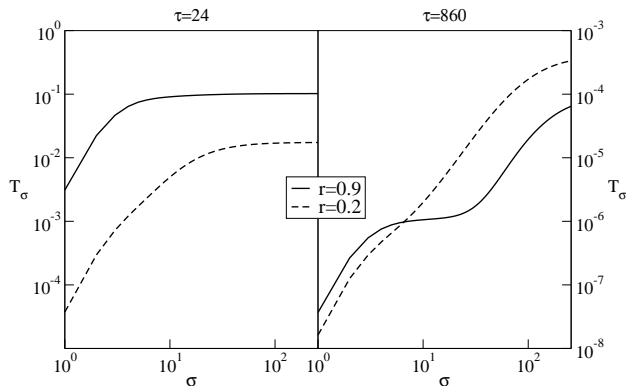


Fig. 16. The scale dependent temperature, T_σ , defined as function of the coarse graining size σ for $\tau = 24$ (incoherent regime) and $\tau = 860$ (correlated regime for both choices of r): the system is the same of figure 8. In the correlated regime the more elastic case presents a plateau at intermediate wavelengths, indicating a well defined *mesoscopic* temperature, and therefore a clear separation between the microscopic and the macroscopic scales.

absence of scale separation between microscopic and macroscopic fluctuations in the strongly inelastic regime [46].

6 Conclusions

We have analysed essentially three different problems with a strong interconnection, in the framework of the physics of cooling granular gases. Our first step (IMM) was to demonstrate that a simplified 1D version of the Boltzmann equation for inelastic gases can be exactly solved by a $P(v)$ with power law tails. However, realistic granular systems never show such large tails: the key feature that must be added to this oversimplified model is a realistic topology. Therefore our second step (ILMM, $d = 1$) was to embed the IMM on a 1D lattice. The $P(v)$ changes dramatically and becomes identical to those measured in MD simulations, also in the velocity-correlated stage. Moreover, the ILMM allows for a study of spatial correlations, resulting in shock-like structures very similar to the one observed in MD and strong analogies with the MD structure functions. Our last step (ILMM, $d = 2$) has been the passage from $d = 1$ to $d = 2$, which mainly results in the appearance of vortices. Vortices are ubiquitous in granular gases experiments and simulations. The ILMM simply produces vortices as a result of the competition between the parallelizing effect of inelastic collisions and the constraint given by the conservation of total momentum. Moreover, a large set of evidences (energy decay, structure factors, Gaussian velocity pdf's, aging self-correlations, persistence exponent) indicate that the dynamical behavior of the system is compatible with a diffusion equation, even if short scale defects (appearing

as shocks, internal noise and tails *à la* Porod in the structure functions) make this model richer.

References

1. T. Pöschel and S. Luding. *Granular Gases*. Springer Verlag, Berlin, 2000.
2. P. K. Haff. Grain flow as a fluid-mechanical phenomenon. *J. Fluid Mech.*, 134:401, 1983.
3. I. Goldhirsch and G. Zanetti. Clustering instability in dissipative gases. *Phys. Rev. Lett.*, 70:1619, 1993.
4. S. McNamara and W. R. Young. Inelastic collapse and clumping in a one-dimensional granular medium. *Phys. Fluids A*, 4:496, 1992.
5. P. Deltour and J.-L. Barrat. Quantitative study of a freely cooling granular medium. *J. Phys. I France*, 7:137, 1997.
6. T. P. C. van Noije, M. H. Ernst, R. Brito, and J. A. G. Orza. Mesoscopic theory of granular fluids. *Phys. Rev. Lett.*, 79:411, 1997.
7. T. P. C. van Noije and M. H. Ernst. Ring kinetic theory for an idealized granular gas. *Physica A*, 251:266, 1998.
8. T. P. C. van Noije and M. H. Ernst. Cahn-Hilliard theory for unstable granular flows. *Phys. Rev. E*, 61:1765, 2000.
9. E. Ben-Naim, S. Y. Chen, G. D. Doolent, and S. Redner. Shock-like dynamics of inelastic gases. *Phys. Rev. Lett.*, 83:4069, 1999.
10. X. Nie, E. Ben-Naim, and S. Chen. Dynamics of freely cooling granular gases. *Phys. Rev. Lett.*, 89:204301, 2002.
11. J. Wakou, R. Brito, and M. H. Ernst. Towards a Landau-Ginzburg-type Theory for Granular Fluids. *J. Stat. Phys.*, 3:107, 2002.
12. R. Brito and M. H. Ernst. Extension of Haff's cooling law in granular flows. *Europhys. Lett.*, 43:497, 1998.
13. A. Baldassarri, U. Marini Bettolo Marconi, and A. Puglisi. Influence of correlations on the velocity statistics of scalar granular gases. *Europhys. Lett.*, 58:14, 2002.
14. A. Baldassarri, U. Marini Bettolo Marconi, and A. Puglisi. Models of freely evolving granular gases. *Advances Complex Systems*, 4:321, 2001.
15. A. Baldassarri, U. Marini Bettolo Marconi, and A. Puglisi. Kinetics models of inelastic gases. *Math. Mod. Meth. Appl. S.*, 12:965, 2002.
16. A. Baldassarri, U. Marini Bettolo Marconi, and A. Puglisi. Cooling of a lattice granular fluid as an ordering process. *Phys.Rev.E*, 65:051301, 2002.
17. T. Pöschel, N. V. Brilliantov, and T. Schwager. Violation of molecular chaos in dissipative gases. Unpublished (cond-mat/0210058), 2002.
18. J. J. Brey, J. W. Dufty, C. S. Kim, and A. Santos. Hydrodynamics for granular flow at low density. *Phys. Rev. E*, 58:4638, 1998.
19. J. A. G. Orza, R. Brito, T. P. C. van Noije, and M. H. Ernst. Patterns and long range correlations in idealized granular flows. *Int. J. of Mod. Phys. C*, 8:953, 1997.
20. M. Isobe. Private communication.
21. P. C. Hohenberg and B. I. Halperin. Theory of dynamic critical phenomena. *Rev.Mod.Phys.*, 49:435, 1977.

22. G. F. Carnevale, Y. Pomeau, and W. R. Young. Statistics of ballistic agglomeration. *Phys. Rev. Lett.*, 64:2913, 1990.
23. S. F. Shandarin and Ya. B. Zeldovich. The large-scale structure of the universe: Turbulence, intermittency, structures in a self-gravitating medium. *Rev. Mod. Phys.*, 61:185, 1989.
24. A. Barrat E. Trizac. Free cooling and inelastic collapse of granular gases in high dimensions. *Eur. Phys. J. E*, 5:161, 2000.
25. S. Ulam. On the operations of pair production, transmutations and generalized random walk. *Adv. Appl. Math.*, 1:7, 1980.
26. J. C. Maxwell. On the dynamic theory of gases. *Phil. Trans. R. Soc.*, 157:49, 1867.
27. M H. Ernst. Nonlinear model-Boltzmann equations and exact solutions. *Phys. Rep.*, 78:1, 1981.
28. A. V. Bobylev, J. A. Carrillo, and I. M. Gamba. On some properties of kinetic and hydrodynamic equations for inelastic interactions. *J. Stat. Phys.*, 98:743, 2000.
29. M. H. Ernst. Scaling solutions of inelastic Boltzmann equations with overpopulated high energy tails. *J. Stat. Phys.*, 109:407, 2002.
30. E. Ben-Naim and P. Krapivsky. Scaling, multiscaling, and nontrivial exponents in inelastic collision processes. *Phys. Rev. E*, 66:011309, 2002.
31. E. Ben-Naim and P. L. Krapivsky. Multiscaling in infinite dimensional collision processes. *Phys. Rev. E.*, 61:R5, 2000.
32. A. Bobylev, C. Cercignani, and G. Toscani. Proof of an asymptotic property of self-similar solutions of the boltzmann equation for granular materials. *J. Stat. Phys.*, 111:403, 2003.
33. U. Marini Bettolo Marconi and A. Puglisi. Mean field model of free cooling inelastic mixtures. *Phys. Rev. E*, 65:051305, 2002.
34. U. Marini Bettolo Marconi and A. Puglisi. Steady state properties of a mean field model of driven inelastic mixtures. *Phys. Rev. E*, 66:011301, 2002.
35. Vicente Garzó and James Dufty. Homogeneous cooling state for a granular mixture. *Phys. Rev. E*, 60:5706, 1999.
36. D. Benedetto, E. Caglioti, and M. Pulvirenti. Kinetic equations for granular media. *Math. Mod. and Num. An.*, 31:615, 1997.
37. A. Barrat, T. Biben, Z. Racz, E. Trizac, and F. van Wijland. On the velocity distributions of the one-dimensional inelastic gas. *J. Phys. A*, 35:463, 2002.
38. S. McNamara and W. R. Young. Inelastic collapse in two dimensions. *Phys. Rev. E*, 50:R28, 1994.
39. S. McNamara S. Luding. How to handle the inelastic collapse of a dissipative hard-sphere gas with the tc model. *Granular Matter*, 1:113, 1998.
40. G. Porod. *Kolloid Z.*, 124:83, 1951.
41. G. Porod. *Kolloid Z.*, 125:51, 1952.
42. A. J. Bray. Theory of phase ordering kinetics. *Adv. Phys.*, 35:43, 1994.
43. M. Huthmann, J. A. G. Orza, and R. Brito. Dynamics of deviations from the gaussian state in a freely cooling homogeneous system of smooth inelastic particles. *Granular Matter*, 2:189, 2000.
44. H. Nakanishi. Velocity distribution of inelastic granular gas in homogeneous cooling state. Unpublished (cond-mat/0208477), 2002.
45. A. J. Bray, B. Derrida, and C. Godrèche. Nontrivial algebraic decay in a soluble model of coarsening. *Europhys. Lett.*, 27:175, 1994.
46. I. Goldhirsch. Scales and kinetics of granular flows. *Chaos*, 9:659, 1999.